DOI: 10.2478/aucts-2024-0001

ACTA UNIVERSITATIS CIBINIENSIS – TECHNICAL SERIES
Vol. 76 2024

PATIENT-SPECIFIC PNEUMATIC ACTUATED WRIST EXOSKELETON FOR INDUSTRIAL REPETITIVE OPERATIONS

PETRUSE Radu Emanuil
Faculty of Engineering, Department of Industrial Engineering and Management, "Lucian Blaga" University, Sibiu, Romania, radu.petruse@ulbsibiu.ro

FLOREA-TOADER Denisa-Gabriela
Kromberg & Schubert Romania, 550024 Sibiu, Romania, denisagabriela.floreatoader@ulbsibiu.ro

Abstract: *This research highlights the significant impact of robotic exoskeletons on improving industrial operations through the prevention of repetitive strain injuries and increased productivity. Utilizing 3D scanning technology enabled customization of the exoskeleton to fit individual users' an-atomical specifications precisely, enhancing comfort and functionality. The iterative design pro-cess was crucial in refining the exoskeleton, addressing issues like structural weaknesses and sizing problems, leading to the development of prototypes with improved features. Advanced sensors, including flexible capacitive pressure sensors and tactile arrays, allowed for real-time monitoring of user interactions, ensuring optimal pressure distribution and preventing discom-fort. The transition to active support with artificial muscles marks a milestone in wearable robotics development for industrial use, enhancing task efficiency while reducing physical strain on workers. Future research should focus on further optimizing the exoskeleton's design for enhanced comfort and functionality, including refining artificial muscle dimensions and materials, and integrating more advanced control systems for improved adaptability.*

Key words: *Patient-specific, wrist exoskeleton, soft robotics, repetitive tasks*

1. INTRODUCTION

Digital health and safety monitoring are concepts that target all industries in the world, aiming to improve the quality of work and increase productivity. These digital initiatives are constantly becoming more advanced. At the same time, consumer-facing digital technologies, such as mobile devices and wearable sensors, are widely present. Thus, it facilitates data collection on almost all aspects of individual lifestyles and behaviours, with an unprecedented potential to add another perspective on repetitive actions within the professional environment. If the health of employees is at a critical point, due to the conditions during the activity, the costs associated with medical care are charged, which is a significant concern from the point of view of a financial perspective. [1]

On the other hand, advances of robotic exoskeleton systems for assisting the individual in movements was to restore the mobility of limbs affected by neurological dis-orders, injuries or surgical procedures [2]. Exoskeletons now also support basic operator functions in repetitive tasks in production plants [3]. The adaptability of the mechanism depending on the individual and the type of movements is a huge challenge, from this point of view, the real-time feedback given by the device has a remarkable impact in improving its functions. The evolution of technology and industry has led to combining several fields of activity, thus creating robotic equipment and devices. Capitalizing on elements of medicine, starting in 1990, mechanisms have emerged that first aimed at faster medical recovery, after various surgical procedures. One of the first studies on of robot-assisted therapy was based on the MIT-Manus system, developed at the Massachusetts Institute of Technology, with the purpose to rehabilitate the upper extremities [4]. This exoskeleton included joints at the shoulder, elbow and wrist, actuated with the help of motors, as well as sensors, in order to execute the natural movements of the arms. The data recorded with the help of sensors was transmitted to the computer's control system to be processed, resulting the level needed for assistance, but also the resistance necessary for movement. This device incorporates the concept of flexibility, as such, depending on the individual, the complexity of the exercises can be adapted according to different needs. When signalling improper movements, the user received visual or auditory indicators as feedback, through which he could correct his movements [5].

Recent innovations in the field focus on the development of systems, devices and methodologies designed to support users' arms. These innovations are designed to facilitate support for one or both arms, while simultaneously providing considerable freedom of movement. Thus, they allow users to engage in various activities for extended durations while keeping one or both arms in an extended position, which is essential for the efficient execution of multiple tasks.[6–8]

Illustrated in Figure 1, the VOSViewer Network Visualization Map [9] showcases a snapshot of the prevailing trends and terminologies relevant to wrist exoskeleton, where terms such as "exoskeleton (robotics)," "patient rehabilitation," "wrist," and "human" are displayed in the centre of the map, underscoring their importance and frequency within the field, thus validating the initial database search. Moreover, trends towards exoskeleton device are observable through keywords highlighted in light green and yellow, emphasizing newer research directions. These visual depictions serve to offer an over-view of the primary subjects and their interconnectedness within this field.

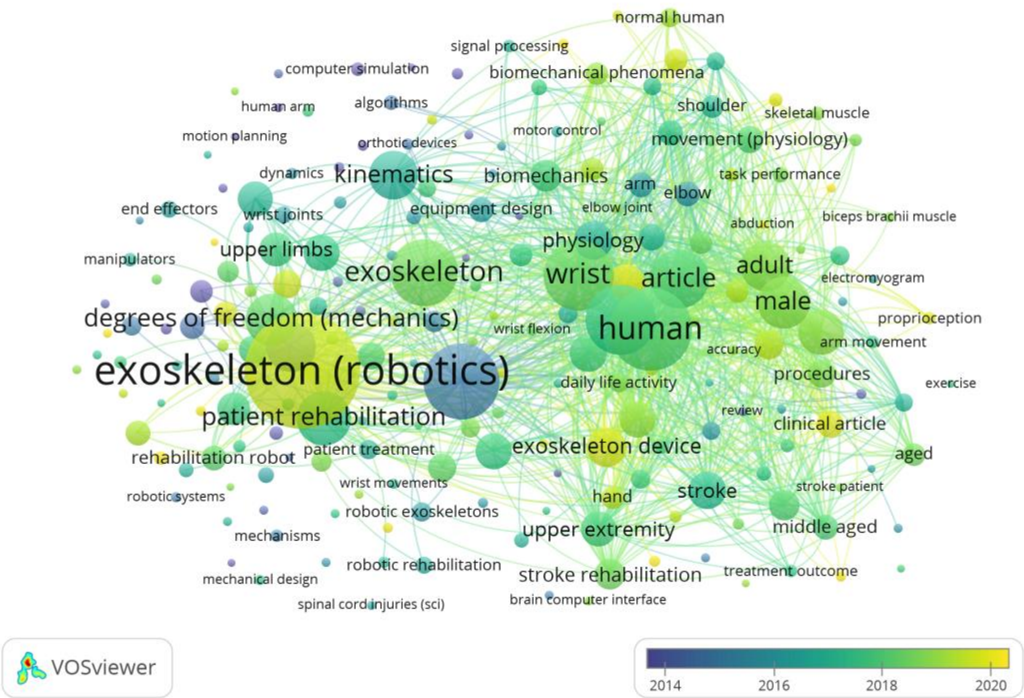

Figure 1. VOSViewer network visualization map for wrist exoskeleton

To better understand the development requirements of a patient-specific wrist exoskeleton actuated by soft robotics, we need to investigate the functional advances of upper limb rehabilitation devices based on robotic technology. The most comprehensive categories of limb support devices offer the following types of movement assistance: active, passive, haptic, and coaching.

1. Active devices

They provide active support for movement and are equipped with at least one actuator, thus allowing motion to be generated. However, in active devices, we can have a range of passive repetitive exercises, due to active joint movements, but which do not require the effort of the person. It is not mandatory to apply active assistance to resist the subject's movements, to improve his strength or for the person to follow the desired trajectory. [10]

2. Passive devices

The main feature that distinguishes an unoperated or passive device lies in its inability to generate movement. The passive devices are equipped with actuators/motors that pro-vide only resistive force. This type of actuator requires a lower energy level and has a lower cost compared to robust actuators used for active assistance. [10]

3. Haptic devices

Haptic equipment falls into the category of systems that interact with the beneficiary through the sense of touch. They are similarly divided into active or passive categories, according to how they are operated. Haptic devices are evaluated independently within their classification, of the main function of provoking or opposing resistance to movements, but rather in providing tactile sensations to the user. [11]

4. Coaching devices

Coaching devices are equipped with sensors, they function as input interfaces for collaboration with therapeutic games in the virtual reality environment, or for telerehabilitation, in other words, remotely monitored therapy. The implementation of coaching systems by identifying movement based on video images (e.g. Microsoft Kinect) would be included in this category, with the mention that any mechanical component in direct contact with the beneficiary is missing. These devices, which are not involved in generating forces in upper limb rehabilitation, nevertheless provide a distinct type of feedback.[12]

To investigate the current state of research on wrist exoskeletons, an extensive literature search was conducted across multiple digital databases, including Scopus (631 results), PubMed (186 results), and Web of Science (593 results). The primary keywords used were "exoskeleton" and "wrist," resulting in 817 unique full-text articles out of 1,407 initially identified. The process of identification, screening, eligibility, and inclusion of 16 relevant articles is detailed step-by-step in the PRISMA[13]diagram (Figure 2) which visually summarizes this methodology, illustrating the flow from initial identification to the final inclusion of studies. This structured approach ensures a comprehensive and systematic review of the literature on wrist exoskeletons.

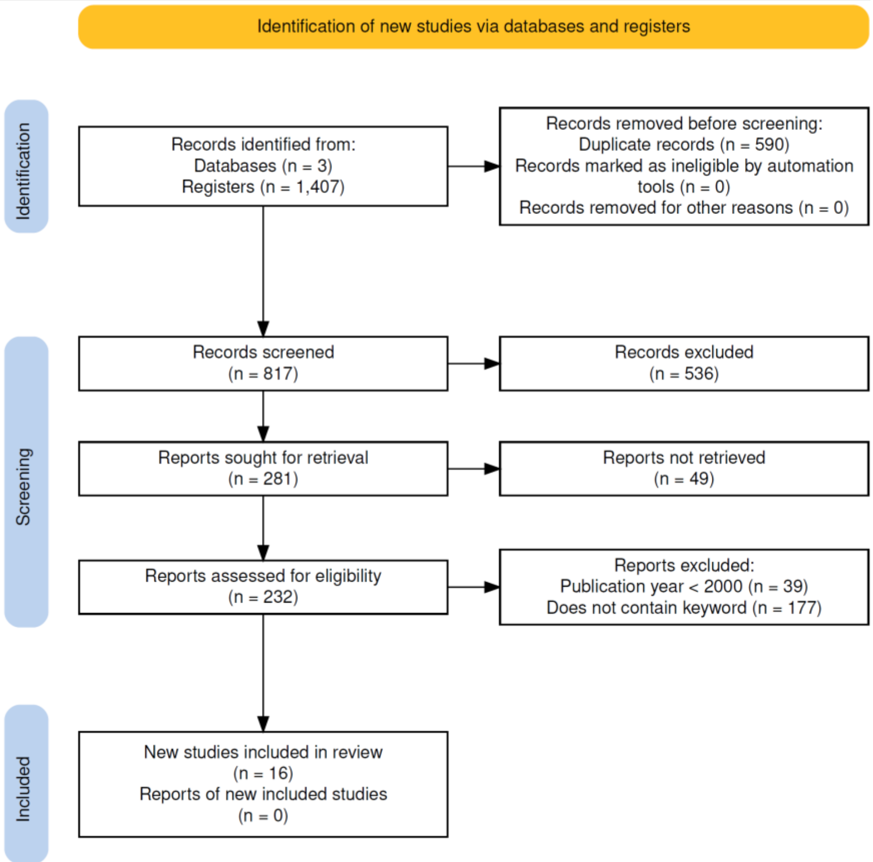

Figure 2. PRISMA diagram presenting state of research screening process.

\

To summarizes key design requirements on wrist exoskeletons from the research studies identified with the PRISMA methodology we have created table 1. Each row represents a different study, detailing the movement assistance type (e.g. active, passive, coaching) and actuation (e.g., artificial muscles), the power source, control mechanisms, and sensor types used. It also includes information on the location of installation and degrees of freedom (DoF), device destination, and whether the device is personalized for each patient. This organized comparison provides a comprehensive overview of the methodologies and technologies employed in the field, facilitating a deeper under-standing of the current research.

Table 1. Summary wrist exoskeleton designs extracted from key studies

Research identifier	Assistance type (active/passive) and actuator category	Power source	Exoskeleton control sensor type	Location of installation and DoF	Device destination	Patient-specific (Yes/No)
Ridremont et al.[14,15]	Coaching Soft actuators	Pneumatic	Flexible sensors installed on external hand and wrist sensor glove	Wrist & fingers DoF: 5 for fingers and 1 for the wrist	Rehab	No, but it fits various sizes
Singh et al. [16]	Active Soft actuators	Pneumatic	X	Wrist DoF: 1 (flexion extension)	Movement assistance - under development	No
Jeong et al. [17,18]	Active SMA (shape memory alloy) Muscles	SMA temperature actuated	X	Wrist DoF: 2 (flexion extension + radial and ulnar deviation)	Movement assistance- under development	No, but it fits various sizes
Nobaveh and Caasenbrood [19]	Semi-active with a passive balance beam Vacuum soft actuators	Vacuum	X	Wrist DoF: 1 (flexion extension)	Movement assistance - under development	No, but it fits various sizes
Chiaradia et al. [20]	Active Planetary gear drive pulley	Electric	9 DoF inertial measurement unit (IMU) and a load cell	Wrist and forearm DoF: 1 (flexion extension)	Movement assistance - under development	Yes
Syafeeq Lone et al. [21]	Active Soft actuators and servomotor	Pneumatic and electric	X	Wrist & thumb DoF: 1 for thumb and 1 for the wrist	Rehab	No, but it fits various sizes
Liu and Takeda [22]	Passive	X	X	Wrist and forearm DoF: 1 (flexion extension)	Rehab	No, but it fits various sizes
Yuejun Xu [23]	Active Soft actuators	Pneumatic	X	Wrist DoF: 1 (flexion extension)	Rehab	Incomplete

Li et al. [24]	Humanoid testing platform	Electric	2 IMUs	Wrist and forearm DoF: 1 (flexion extension)	Rehab	Incomplete
Wang et al. [25]	Coaching Soft actuators	Pneumatic	Flexible sensors installed on external hand and wrist sensor glove	Wrist & fingers DoF: 5 for fingers and 1 for the wrist	Rehab	No, but it fits various sizes
Ang and Yeow [26]	Active Soft actuators	Pneumatic	X	Wrist DoF: 1 (flexion extension)	Rehab	No, but it fits various sizes
Choi et al. [27]	Active Planetary gear drive pulley	Electric	X	Wrist and forearm DoF: 1 (flexion extension)	Rehab and movement assistance - under development	No, but it fits various sizes
Bartlett et al. [28]	Active Soft actuators	Pneumatic	X	Wrist and forearm DoF: 2 (flexion extension + radial and ulnar deviation)	Rehab	No, but it fits various sizes
Andrikopoulos et al. [29]	Active Soft actuators	Pneumatic	Force sensitive resistors	Wrist and forearm DoF: 2 (flexion extension + radial and ulnar deviation)	Rehab	No, but it fits various sizes

As resulted from the literature review, a central problem associated with the clinical configurations of these equipment include inefficient human-robot interaction (HRI), static design, and limited physiologist perceptions. As a result, another focus of research in the field of rehabilitation robots is currently oriented more toward optimizing clinical settings. In the development of rehabilitation devices, at least three objectives should be considered for clinical trials: compliance with surveillance requirements, in line with their research and safety guidelines; synthesizing data on the clinical or financial benefits of using the device compared to existing rehabilitation concepts; providing clinical evidence on the efficacy of the device for different categories of individuals and professional groups. [16]

The device presented in this study, a patient-specific wrist exoskeleton actuated by soft robotics, is an evolution derived from these foundational medical recovery devices. Initially inspired by the pioneering work of systems like the MIT-Manus, our exoskeleton harnesses the same principles of adaptive assistance and real-time feedback. While similar devices were primarily focused on rehabilitating the upper extremities of patients with neurological disorders or post-surgical conditions, our exoskeleton is designed to support manual labour industrial operators. By incorporating advancements in soft robotics and wearable sensor technology, we have adapted the therapeutic benefits of medical exoskeletons to address the repetitive strain injuries commonly faced by workers in industrial settings. This transition from medical recovery to occupational support highlights the versatility of exoskeletal systems and their potential to enhance both health and productivity in various environments.

2. MATERIALS AND METHODS

Identifying the optimal trajectories for arm extension movements is a real challenge. In practice, optimal control models are used, based on arm dynamics, also allowing the incorporation of muscle functioning constraints and muscle stimulation. The results indicate a significant correspondence between the optimal trajectories obtained and the experimental data.

2.1. Wrist kinematics

The human arm can be conceptualized as an articulated mechanism with seven degrees of freedom, thus characterizing itself as a redundant kinematic system. In daily practice, individuals use this kinematic redundancy to achieve arm configurations that maximize comfort and efficiency in executing various handling tasks [30]. This aspect emphasizes the importance of rigorous biomechanical design adapted to the physiological needs of users in the development of exoskeletal devices.[31]

There are three joints associated with spherical wrist movements. The first of these manages the pronation and supination movements of the upper arm, while the other two are responsible for the radioulnar deviation axis and the flexion/extension of the wrist. Pronation and supination movements are types of rotations of the forearm and hand, which involve a change in the position of the palms[31]. Pronation is the movement by which the palm is rotated to face down or towards the back of the body. During pronation, the radius (one of the two long bones of the forearm) rotates over the ulna so that they cross. This causes the palm to turn downwards, with the fingers facing the ground when the arm is extended [32]. Supination is the opposite of pronation and refers to the rotational movement of the forearm and hand so that the palm is facing upwards or towards the face of the body. During supination, the radius rotates back to its position parallel to the ulna, which causes the palm to turn upwards.[32]

These movements are essential for the daily functioning of the hands and arms, allowing for a wide range of actions, from grasping objects to performing more complex movements. The direct solution to best reproduce the movements of the human arm lies in varying the angles of the exoskeleton joints. In contrast, the reverse solution involves determining the angles of the device's joints based on the terminal position.

The wrist joint is undoubtedly one of the most differentiated sections of the musculoskeletal system. The wrist joint is made up of eight carpal bones, proximal carpal row (PCR) and the distal carpal row (DCR), which, in combination with the two bones of the forearm, the radius and the ulna, form its structure. The movement of the wrist joint is initiated by the muscles of the forearm, and the strong and short ligaments ensure the stability of the wrist [33]. All these components are essential for the functioning of the wrist joint, as these structures allow for the mobility and sustainability of the wrist. Function-ally, carpal movement varies within each row, especially within the proximal carpal row (PCR). The bones in the distal carpal tract (DCR) act as a functional unit. Under an axial load, the distal carpal row tends to rotate. It is essential to understand the scientific foundations, as well as the clinical relevance of the functional kinematics of the wrist joint, defined by those movements necessary to perform everyday activities with high demands. [34]

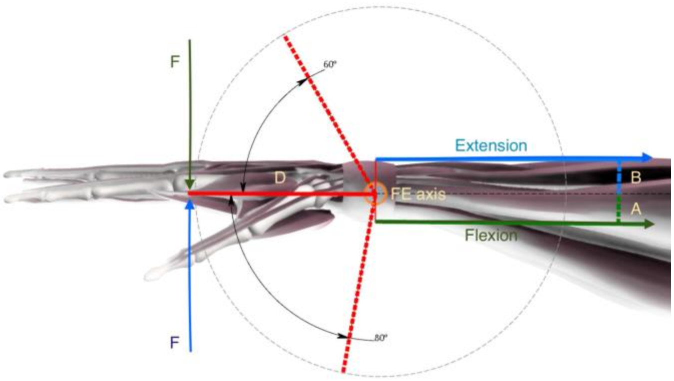

(a)

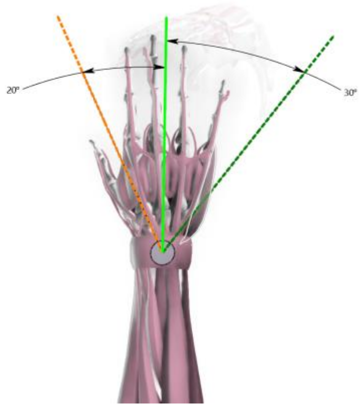

(b)

Figure 3 Flexion-extension and radial-ulnar deviation.

Traditionally, it has been defined in terms of two orthogonal anatomical axes: the flexion-extension (FE) axis and the radial-ulnar deviation (RUD) axis [35]. Starting from a straight wrist, the directions of rotation of the wrist are represented in figure 3 where flexion-extension movements can vary between 0-80° (flexion) 0-60° (extension), and radial-ulnar deviation movements 0-20° (radial) 0-30° (ulnar). Everyday activities tend to have 5–10° to 30–35° for flexion-extension and 10° to 15° for radial-ulnar deviation. Generally speaking, the wrist joint is considered to have two degrees of freedom [36]. Modelling the wrist joint using a simplified static mechanical model is a very accessible possibility. Mathematical predictions can be made using various modelling techniques to obtain information that is not otherwise available [37]. It has already been stated that computational models will become fundamental tools in biomechanics to address future research questions and clinical applications. [38]

2.2. Patient-specific wrist exoskeleton design

To create a patient-specific exoskeleton, we utilized the Artec Leo 3D scanner to obtain precise anatomical data from the user. This process involved capturing detailed measurements of the user's wrist and surrounding areas to ensure an exact fit of the exoskeleton. After the scanning process, the scan sections were fused together using Artec Studio 15 software. Initially, 3D noise was filtered out, retaining only the surfaces of interest. The second step involved aligning multiple scans to ensure comprehensive coverage from various angles. This was followed by a global registration of points and surfaces, merging them while eliminating noise and unwanted points from the data (figure 4a). In the third step, the scans were fused to create a solid and continuous 3D model. The polygonal structure was optimized, simplifying the model while preserving necessary details. Textures were then applied to enhance realism (figure 4b). The entire acquisition and filtering process took approximately four minutes, resulting in a usable 3D point cloud model through a semi-automatic procedure.

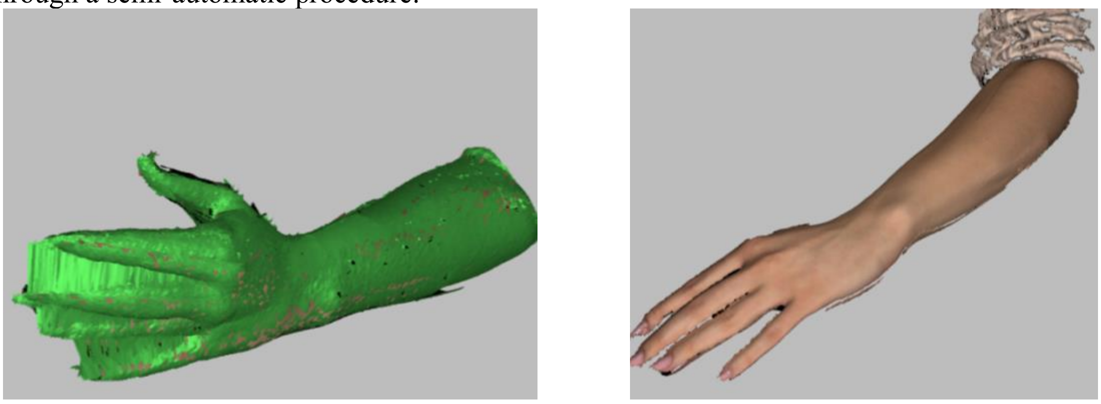

(a) (b)

Figure 4 3D scanning result

The generated 3D model was exported in. stl format and imported into Geomagic Design X v2019.0.3 for further refinement. In this software, holes were filled, surfaces were healed, and the point cloud model was converted into a surface-based 3D model in IGS format. Although the initial results were promising, they contained minor flaws. These defects were subsequently addressed and corrected using CATIA V5-6R2021 software. Once all defects were cleared and the model was "watertight," it was converted into a volumetric 3D model in STP format using CATIA V5-6R2021. Boolean operations within the Part Design module were employed using this volumetric 3D model to create the negative surface representing the interior of the wrist exoskeleton (figure 5a). To ensure user comfort, this surface was offset by 5mm to accommodate memory foam inside the exoskeleton.

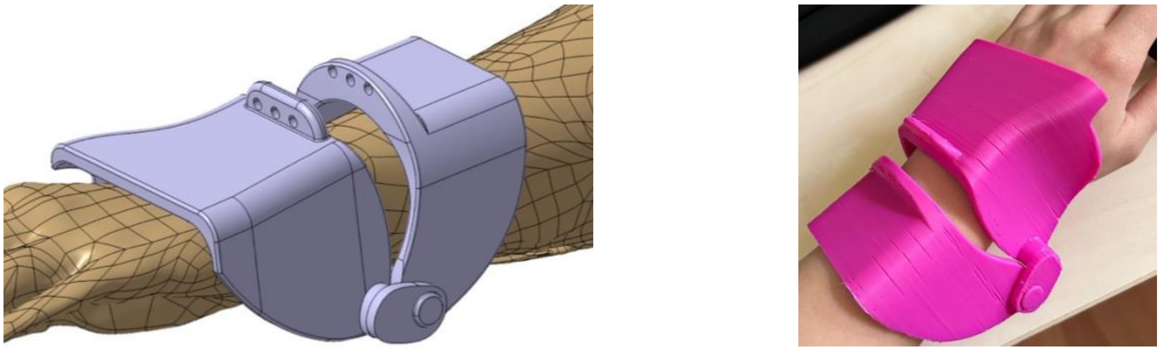

(a) (b)

Figure 5 First wrist exoskeleton prototype development

The first prototype fabricated was designed to test the accuracy of the interior surface in relation to the user's wrist anatomy. This initial device featured a single revolute joint, providing 1 Degree of Freedom (DoF) for flexion-extension movements. The design included a forearm piece and a wrist piece, connected by flexible elements with a circular cross-section. The assembly process involved gently pressing the ears of the forearm part to secure the components together (figure 5b). Upon completing the 3D model of the first prototype, the design was realized through 3D printing. It was conceived as a passive exoskeleton, requiring the user to stretch three bands, which were 3D printed from flexible thermoplastic polyurethane (TPU) material.

After producing the physical model, several observations and conclusions were made:

Structural Weakness: The wall thickness of the side revolution joint was insufficient, leading to breakage after repeated use.

Oversized Dimensions: The overall dimensions of the device were too large, necessitating a reduction in size for better fit and functionality.

Thumb Movement Restriction: The length of the wrist piece interfered with the thumb's range of motion, hindering its natural movement.

Limited Flexibility: The prototype exhibited limited movement due to excessive rigidity, impacting the device's effectiveness in mimicking natural wrist movements.

These findings highlighted critical areas for improvement, providing insights for the subsequent iterations of the exoskeleton design.

Taking into account all the necessary optimizations and changes identified from the first prototype, the design of the 3D model was reinitiated. This iteration focused on achieving precise accuracy by involving the whole negative model of the hand, ensuring that the exoskeleton dimensions were tailored to each individual user. In addressing the rigidity issues from the first prototype, the design incorporated a metal spherical joint to replace the previous side joint. The metal spherical joint (REV-49-1561-PK4 model [39]) has a 9mm ball with a ball-hole suitable for M3 clearance and a threaded M3 rod. The load rating for this spherical rod is 2.2KN. This spherical joint closely mimicked the actual joint in the wrist, allowing for a greater range of natural movements (figure 6). The movement limits are in conformity with ergonomic daily use [40], ensuring that the wrist joint is not adversely affected. As depicted in Figure 6a, the extension limit is 30°, and the flexion is limited by the length of the artificial muscle, although the exoskeleton can facilitate movement beyond human anatomical possibilities (Figure 6b). The radial deviation is approximately 13° (Figure 6c), and the ulnar deviation is 18° (Figure 6d), both within normal ergonomic use.

Additionally, the device was designed to be operated with pneumatic artificial muscles, consisting of rubber tubes with a diameter of 8mm. The artificial muscles provided the necessary actuation, enhancing the device's functionality and responsiveness.

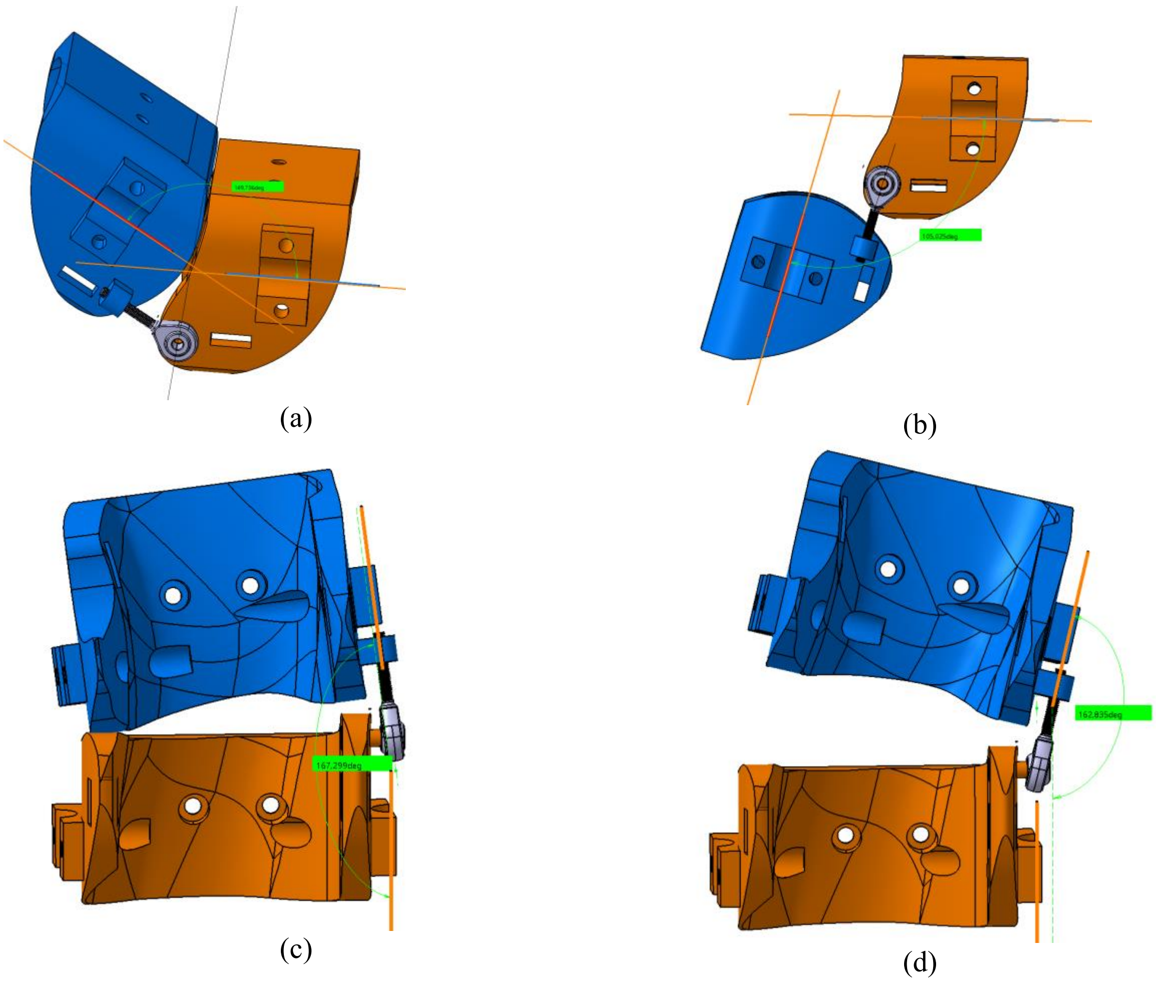

Figure 6 Spherical joint kinematic limits: a-flexion; b-extension; c-radial; d-ulnar

This second prototype incorporated several key improvements:

Enhanced Flexibility: The metal spherical joint allowed for more natural wrist movements, providing three DoF, of which two are utilized: one for flexion-extension and one for ulnar-radial deviation. This significantly improved the range and fluidity of movements compared to the previous design.

Customized Fit: Utilizing a complete negative 3D model ensured that the exoskeleton was precisely tailored to the user's specific wrist dimensions. This customization enhanced both comfort and effectiveness, ensuring the device did not restrict finger movements while providing a secure fit.

Improved Actuation: The inclusion of artificial muscles provided a more sophisticated and responsive method of operation, enhancing the user's ability to perform repetitive tasks with less strain and transforming the exoskeleton from a passive device to an active one.

These enhancements addressed the shortcomings of the first prototype and marked significant progress towards developing a practical and effective patient-specific wrist exoskeleton.

2.3. Wrist Exoskeleton Control Sensors

For detecting the interaction between the user's wrist and the exoskeleton, several types of pressure sensors can be considered, each offering unique advantages depending on the specific application requirements. For this this study we analysed several technologies, as presented in table 2.

Table 2. Pressure sensors comparison

Sensor type	Description	Advantages	Disadvantages
Force sensing Resistors	These are thin and flexible force sensors that can be easily integrated into wearable devices.	They have a thin profile, are flexible, and are easy to install on curved surfaces like a wrist.	They are limited to detecting force at discrete points rather than providing continuous pressure distribution.
Capacitive	These sensors	High sensitivity,	They can be sensitive

Pressure Sensors	measure pressure changes based on the capacitance variation between two conductive plates.	can be made very thin, and capable of measuring a wide range of pressures.	to environmental changes like humidity.
Piezoelectric Sensors	These sensors generate an electrical charge in response to mechanical stress.	High sensitivity and good for detecting dynamic pressure changes.	Less effective for static or slowly changing pressures.
Strain Gauge Sensors	These sensors measure the strain (deformation) in the material to which they are attached.	High accuracy and can measure distributed pressure when integrated into a flexible matrix.	They require careful calibration and can be sensitive to temperature changes.
Optical Pressure Sensors	These sensors use changes in light properties (such as intensity or wavelength) to measure pressure.	High sensitivity, immune to electromagnetic interference, and can be made very small.	They can be complex to integrate and require careful alignment.
Tactile Pressure Sensors (Tactile Arrays)	These consist of arrays of small pressure sensors that can detect pressure distribution over an area.	Can provide detailed pressure maps, useful for detecting pressure distribution.	More complex and potentially more expensive than single-point sensors.

For the developed exoskeleton, tactile pressure sensors (tactile arrays) or flexible capacitive pressure sensors are particularly well-suited. These sensors conform to the curved surfaces of the wrist and provide detailed pressure distribution data, helping to optimize the fit and prevent excessive pressure points from causing discomfort. One suitable option is the FlexiForce A201 by Tekscan[41], a thin and flexible sensor that detects varying pressure levels at discrete points. However, integrating this sensor into the exoskeleton's body may reduce its structural resistance and potentially disturb the user. Another viable option is the flexible pressure sensing pad "Conformable TactArray"[42] from PPS. This sensor pad is approximately 1mm thick, made from soft, conductive cloth, and captures pressure distribution between two objects in direct physical contact. The Conformable TactArray can accommodate varying degrees of curvature and provides accurate, repeatable data even when wrapped around irregular shapes.

By selecting the appropriate type of pressure sensor and integrating it into the exoskeleton design, the interaction between the user's wrist and the device can be effectively monitored, ensuring both comfort and functionality.

2.4. Numerical validation- finite element analysis

After validating the kinematic capabilities of the designed exoskeleton, it was crucial to ensure that the physical prototype could withstand the operational loads. To achieve this, we employed a static finite element analysis (FEA) using the analysis and simulation module in CATIA V5-6R2021.

First, we needed to identify the required loads by calculating the muscle forces, in this case the flexor muscles, synthesized according to the free body diagram shown in figure 7. This force is also required for the design of the artificial muscles which will be installed on the wrist exoskeleton. For this case study we used a weight of approximately 10kg which is translated to a force of 100N.

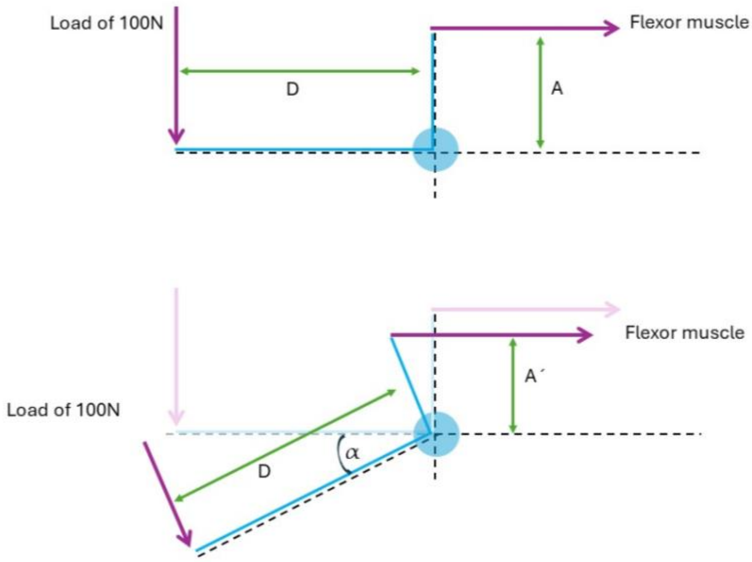

Figure 7 Free body diagram for the flexor muscles

The free body diagram for the changing lever arm of the synthesized flexor muscles in wrist extension with a load of 100 N applied to the third metacarpal bone is depicted in Figure 3a and 7. Here, D represents the lever arm of the applied load, A is the lever arm of the synthesized flexor muscles, and A**'** is the new lever arm according to the wrist's extension angle.

To obtain the flexor muscles required force, the following equation must be solved:

$$F \cdot D = FM \cdot A \text{ [43]}$$

Where F is the external load in [N], D is the lever arm of the external load, FM is the synthesized muscle force of the flexor muscles, and A is the lever arm of all the flexor muscles. In order to be able to calculate the force, F and FM must be separated:

$$FM = (F*D)/A \text{ [43]}$$

The change in the position of the arm depends on the angle between the neutral position and the current position, and this can be calculated with:

$$A` = A \cdot \cos\alpha \text{ [43]}$$

To calculate the resultant reaction force of the joint, the forces in the x and y directions must be summed separately. For the x-direction, the following must be calculated:

$$FX = \sum FX1 + FX2 + \cdot\cdot\cdot + FXn = 0 \text{ [43]}$$

In this case, only one external force FE is applied:

$$FX = FE* \sin\alpha \text{ [43]}$$

Where FE= 100N and the angle α is the angle between FE and vertical

For the y-direction, it must be calculated

$$FY = \sum FY1 + FY2 + \cdot\cdot\cdot + FYn = 0 \text{ [43]}$$

And in this case, it's just an applied external force, FE:

$$FY = FE* \cos\alpha \text{ [43]}$$

For the resulting external joint reaction force, it must be solved:

$$FR = \sqrt{Fx^2 + Fy^2}\text{[43]}$$

Muscle forces are calculated separately and will be considered for the full load of the joint.

Considering that α is set to 30 degrees and FE set to 100N we have the following results:

$$FX = 100 * \sin(30°) = 100 * 0.5 = 50N$$

$$FY = 100 * \cos(30°) = 100 * \frac{\sqrt{3}}{2} = 86.6N$$

$$FR = \sqrt{2500 + 7498.56} =\approx 100N$$

The resultant external joint reaction force FR is approximately 100 N. This confirms that the theoretical and practical calculations align well under the given conditions.

To ensure the structural integrity of the exoskeleton prototype, we performed a finite element analysis using the simulation module in CATIA V5-6R2021. The first step was to define the material properties of the 3D-printed parts. For the components made of Acrylonitrile Butadiene Styrene (ABS) material, the following values are used: Yield strength of 44.7MPa and Young's modulus of 2.04GPa [44]. The spherical joint was defined as stainless steel, utilizing mechanical characteristics from the CATIA materials database. To enhance the accuracy of the analysis, the finite element mesh size was reduced in the areas of interest. Constraints were applied on the surfaces where the artificial muscles are mounted, defining the interaction between components as contact with limited sliding. These constraints were applied between the two main components of the device and the screws fixing the spherical joint. A radial force of 100 N, distributed on the fixing surface of one of the lateral artificial muscles, was applied to the side of the exoskeleton (figure 8a). The critical area identified was around the spherical rod fixture. The resulting Von Mises stress was concentrated in this area. The maximum stress value obtained from the finite element analysis was 36.5 MPa (figure 8b), which is well below the maximum permissible limit for ABS material of 44.7 MPa. This indicates that the material's yield limit was not reached, demonstrating the prototype's structural robustness under the given load. Moreover, considering that the applied force exceeds the typical operational force, and that the nuts fixing the rod to the exoskeleton were not included in the analysis, we can confidently conclude that this prototype meets the design requirements. This validation confirms the exoskeleton's ability to withstand operational stresses, ensuring its durability and reliability in practical applications.

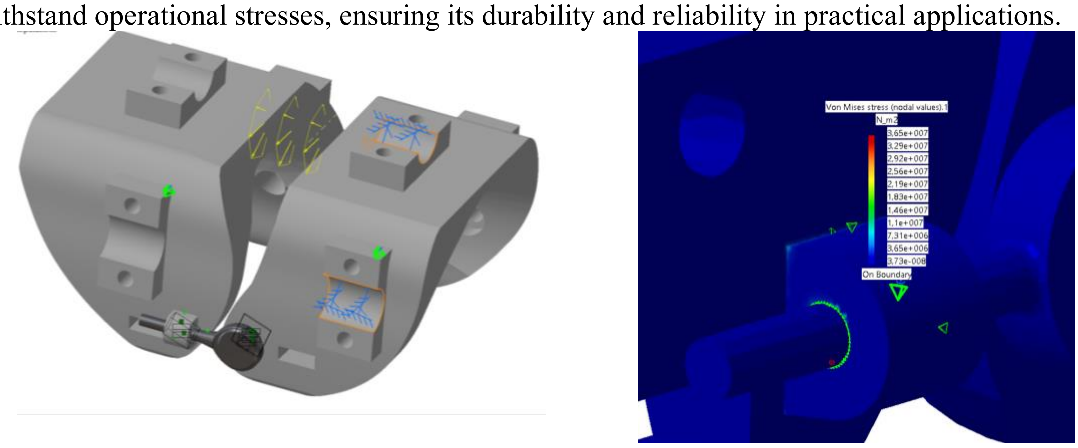

(a) (b)

Figure 8 FEA setup and result

2.4. Artificial Muscle Development

To create the artificial muscles that actuate the wrist exoskeleton we inspired from Rusu et al. [45]. For the core of the artificial muscles 8mm diameter silicone tubes with a wall thickness of 1.5mm are used (figure 9a). To enhance their durability and functionality, we encased the silicone tubes in flexible sleeves commonly used in automotive cable protection, known as "braided sleeves" (figure 9b). These braided sleeves are made of PET (polyethylene terephthalate), a material renowned for its robustness and they can withstand a wide range of temperatures, from -50 to 150 degrees Celsius, making them ideal for demanding environments. These sleeves offer excellent protection against abrasion, moisture, and chemicals, ensuring the longevity and reliability of the artificial muscles. Furthermore, these sleeves are highly flexible and can easily expand to accommodate various cable sizes, allowing for straightforward installation over the silicone tubes.

At each end of the silicone tubes, we installed specialized plugs to facilitate the application of pneumatic pressure and to manage the release of pressure. One end of each tube is fitted with a plug that allows for the application of pneumatic pressure, crucial for the actuation mechanism of the artificial muscles (figure 9b). The other end of the tube can be equipped with a quick release valve, enabling rapid depressurization and allowing for quick adjustments and control of the exoskeleton's movements.

(a) (b)

Figure 9 Artificial muscles components and assembly

By using these components, we ensured that the artificial muscles are not only effective in actuating the exoskeleton but also durable and capable of withstanding the rigorous conditions they might encounter during use. The combination of silicone tubes and PET braided sleeves provides a balance of flexibility and strength, making the artificial muscles suitable for the repetitive and precise movements required by the wrist exoskeleton.

3. RESULTS

The utilization of 3D scanning technology allowed us to generate a high-resolution digital model of the patient's wrist, which was subsequently used to design the custom components of the exoskeleton. By leveraging these precise measurements, we tailored the exoskeleton to the unique morphology of the patient, ensuring optimal comfort, effectiveness, and functionality. This patient-specific approach is critical in enhancing the adaptability and performance of the exoskeleton, as it accommodates individual variations in wrist size and shape, thereby providing better support during repetitive tasks.

The manufacturing parameters for the 3D printing of the device were as follows: a layer height of 0.16 mm, a filling density of 25% using a "Cubic" pattern, a wall thickness of 1.2 mm, and a printing speed of 60 mm/s. The total manufacturing time was 12 hours and 11 minutes, using 104.1 grams of ABS filament (figure 10a).

After 3D printing, the structural improvements between the models were immediately noticeable. The dimensions were significantly reduced, facilitating greater user comfort. The incorporation of a ball joint significantly enhanced the mobility of the exoskeleton. The wrist component was redesigned to ensure that the thumb movement was no longer impeded, and the eccentricity supporting the joint screw was optimized for better dimensions (figure 10b).

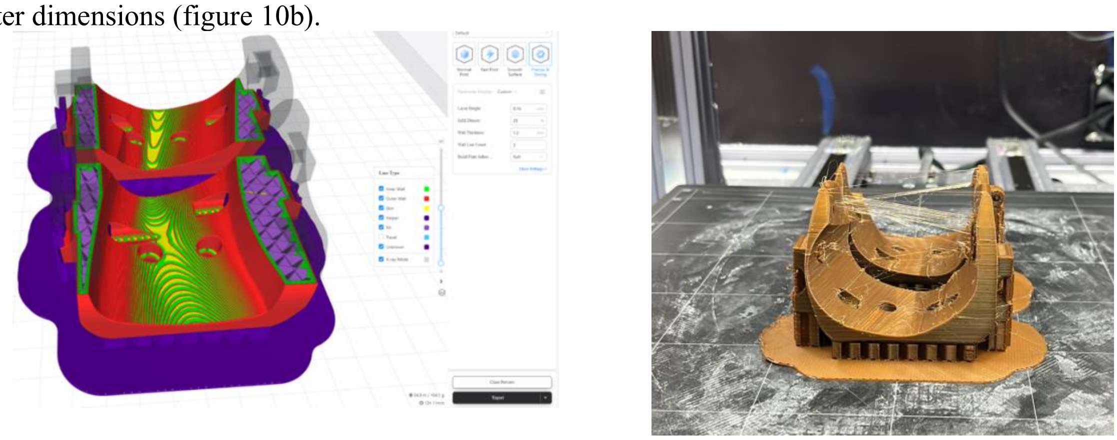

(a) (b)

Figure 10 Fabrication setup (a) and result (b)

Despite the considerable improvements in the second prototype, an issue was identified with the eccentricity supporting the joint screw, which caused the model to shift to one side due to the joint dimensions. To address this, a protrusion was added to the mounting surface of the ball joint, and the eccentricity was shifted by 3 mm, resulting in prototype number 3. This adjustment ensured that the forearm piece was properly aligned with the wrist piece, facilitating correct use during movement. Additionally, the boss added to the mounting surface successfully distanced the ball joint body from the part, allowing for the proper functioning of the sphere.

Following these adjustments, the exoskeleton was assembled with 6 horseshoes, 12 screws, 12 nuts, and 3 artificial muscles (figure 11a-b).

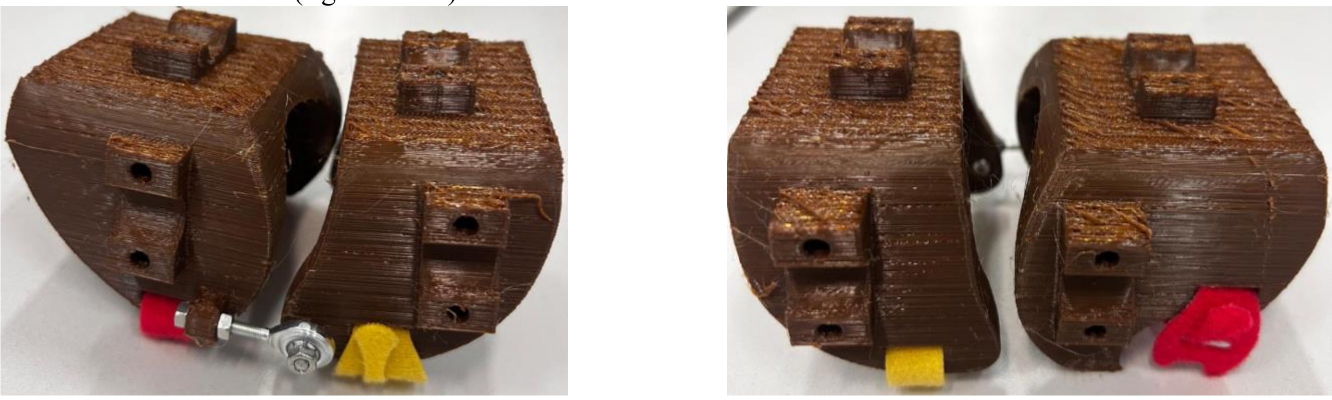

Figure 11 3D printed patient-specific exoskeleton assembled components

The device's capabilities were carefully calibrated to ensure they did not exceed the wrist's natural range of motion, guaranteeing that the musculoskeletal system remains protected from any unwanted injuries due to movement patterns that exceed orthopaedic regulations regarding extreme joint movements. To achieve this, we measured the force generated by the artificial muscles at various pressures. For this experiment, the Galdabini Quasar 25 bench top universal test machine in conjunction with the Graphwork control software is utilised. To secure the artificial muscle in the testing machine's grippers, a 3D printed device was manufactured, employing the same horseshoe used to attach the muscles to the wrist exoskeleton (figure). While the experiment aimed to test the muscles to the point of failure, the maximum pressure generated by the compressor (8.5 Bar) was insufficient to destroy the muscles, demonstrating their robustness.

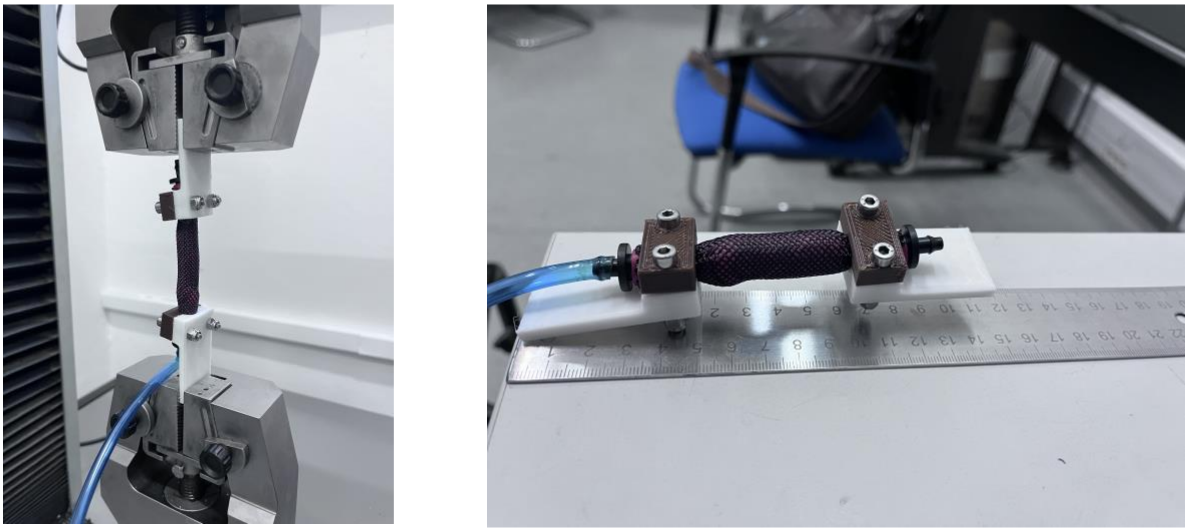

(a) (b)

Figure 12 Artificial muscle force testing setup (a) and travel limit measurement (b)

During this experiment we were also able to measure the travel limit of the artificial muscle. For a pressure of 6 Bar the artificial muscle contracted by approximately 20mm. In order to increase the travel of the artificial muscle, a sleeve with a larger diameter is required.

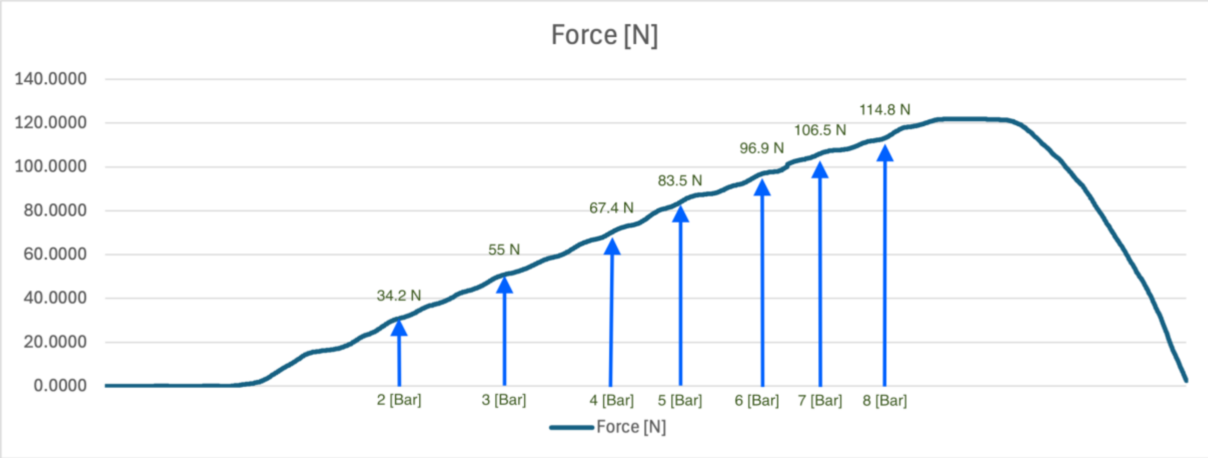

Figure 13 Artificial muscle force at different pressure

As depicted in figure 13, the maximum traction force generated by the artificial muscle exceeded the requirements, of 100N calculated during the exoskeleton design phase.

As demonstrated in Figure 14a and 14b, the flexion-extension movement was successfully performed with the assistance of a compressor, effectively supporting the wrist during repetitive tasks. Although the manufactured artificial muscles can withstand pressures up to 8.5 Bar, this experiment was conducted with a pressure of only 4 Bar to ensure user safety. The test revealed a limitation: due to the rigidity and short travel distance of the muscle, the flexion-extension movement is restricted to approximately 20 degrees. Similarly, the radial-ulnar deviation (Figures 14c-f) is limited to around 15 degrees.

As depicted in figure 13, the maximum traction force generated by the artificial muscle exceeded the requirements, of 100N calculated during the exoskeleton design phase.

As demonstrated in Figure 14a and 14b, the flexion-extension movement was successfully performed with the assistance of a compressor, effectively supporting the wrist during repetitive tasks. Although the manufactured artificial muscles can withstand pressures up to 8.5 Bar, this experiment was conducted with a pressure of only 4 Bar to ensure user safety. The test revealed a limitation: due to the rigidity and short travel distance of the muscle, the flexion-extension movement is restricted to approximately 20 degrees. Similarly, the radial-ulnar deviation (Figures 14c-f) is limited to around 15 degrees.

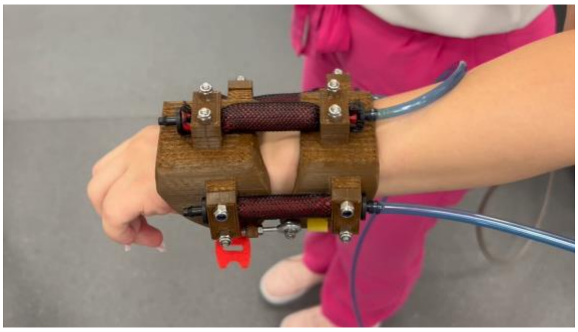

(a)

(b)

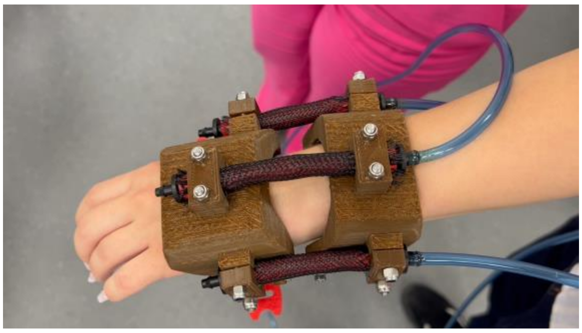

(c)

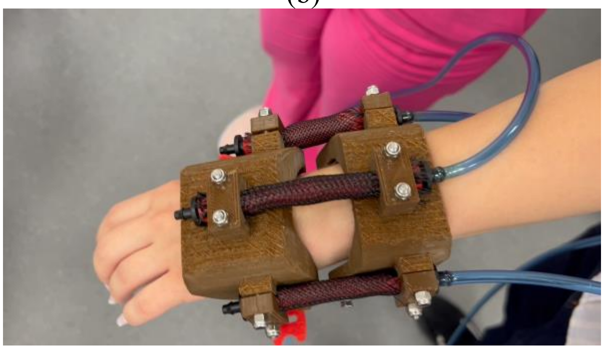

(d)

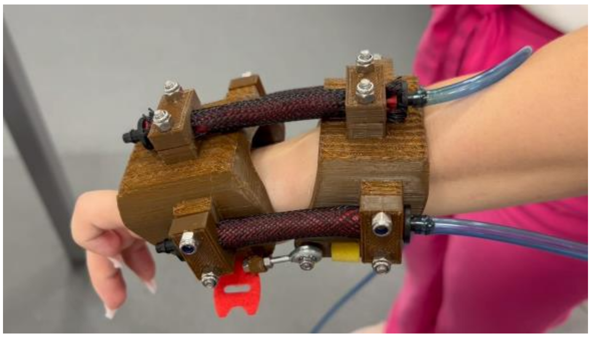

(e)

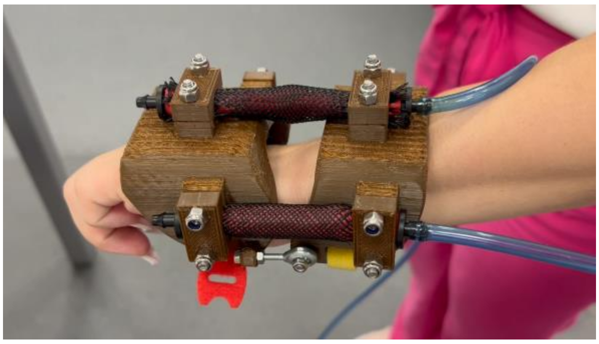

(f)

Figure 14 Wrist exoskeleton actuation at 4 Bar:
a, b-flexion extension; c, d-radial deviation; e, f- ulnar deviation

4. FUTURE RESEARCH

To further enhance the functionality and effectiveness of the wrist exoskeleton, several opportunities for future research and development are proposed. Investigating alternative materials for the exoskeleton structure (e.g. TPU) and artificial muscles that offer better flexibility, durability, and comfort could provide significant improvements. Developing artificial muscles with increased travel distances and reduced rigidity is another key area. Experimenting with different sleeve diameters and materials or exploring new types of actuators such as shape memory alloys (SMAs), could enhance the range of motion and overall performance of the exoskeleton.

Incorporating a wider array of sensors, such as advanced pressure, strain, and motion sensors, would provide real-time feedback on the interaction between the exoskeleton and the user's wrist. This data can be used to fine-tune the device for improved comfort and functionality. Developing sophisticated control algorithms that can adapt to the user's movements and provide more natural and intuitive support is also essential. Machine learning techniques could be employed to predict and adapt to the user's motion patterns, enhancing the user experience. Conducting extensive user trials to gather feedback on the comfort, effectiveness, and usability of the exoskeleton is crucial for iterative design improvements and ensuring that the device meets the needs of a diverse range of users. Performing detailed ergonomic studies will help further understand the impact of the exoskeleton on the user's wrist and overall biomechanics, ensuring that the device supports natural wrist movements without causing strain or discomfort.

Researching and developing compact and efficient power supply systems that can be integrated into the exoskeleton is another important area.

Investigating scalable manufacturing processes that allow for mass customization of the exoskeleton will make it accessible to a broader range of users while maintaining a personalized fit and functionality. Ensuring that the exoskeleton complies with relevant safety standards and regulations by developing fail-safe mechanisms and emergency release systems to protect the user in case of malfunction is also essential.

5. CONCLUSIONS

This study aimed to explore the functionality of devices designed to assist users in improving mobility, focusing on the development and testing of a patient-specific wrist exoskeleton. Robotic equipment, identified as a promising alternative to manual therapeutic interventions, shows potential for the rehabilitation of patients with nervous disorders, enhancing human power and providing robotic assistance. These devices facilitate repetitive and precise movements, both simple and complex, surpassing the capabilities of a therapist without extensive practice. The safety and feasibility of using exoskeletal devices, whether mechanically operated by actuators or not, were also examined.

The research involved the design and manufacture of a patient-specific wrist exoskeleton, involving advanced 3D scanning technology to generate a high-resolution digital model of the patient's wrist. This enabled the precise design of custom exoskeleton components tailored to the unique morphology of the patient, ensuring optimal comfort, effectiveness, and functionality. The personalized approach accommodated individual variations in wrist size and shape, enhancing support during repetitive tasks. Through several iterations, the exoskeleton design was carefully optimized, resulting in a significantly improved prototype. The inclusion of a ball joint enhanced the mobility of movements, and design adjustments ensured that the exoskeleton did not impede thumb movement. Finite element analysis confirmed the structural robustness of the exoskeleton under a radial force of 100 N. Critical stress areas were identified, and the maximum stress value was within the permissible limits for ABS material, ensuring the prototype's durability under operational conditions.

The artificial muscles, constructed from silicone tubes encased in PET braided sleeves, proved to be effective actuators for the exoskeleton, providing the necessary force and durability while withstanding pressures up to 8.5 Bar. For safety reasons, tests were conducted at 4 Bar, successfully performing the flexion-extension movement, although it was limited to approximately 20 degrees due to the rigidity and short travel distance of the muscles. Similarly, the radial-ulnar deviation was restricted to around 15 degrees.

In conclusion, the developed wrist exoskeleton demonstrates significant potential for supporting repetitive wrist movements with patient-specific customization. Further refinement of the artificial muscles to increase their flexibility and travel distance, as well as ongoing adjustments to the exoskeleton design, will enhance its overall performance and user comfort. The integration of advanced pressure sensors will further optimize the functionality, ensuring the exoskeleton meets user needs while preventing unwanted injuries due to excessive movement. Moreover, developing a control system using machine learning algorithms can adaptively assist the user based on their specific movement patterns and needs, further enhancing the device's functionality and user experience.

References

1. Karas, M.; Marinsek, N.; Goldhahn, J.; Foschini, L.; Ramirez, E.; Clay, I. Predicting Subjective Recovery from Lower Limb Surgery Using Consumer Wearables. *Digit Biomark* 2020, *4*, 73–86, doi:10.1159/000511531.
2. Pitzalis, R.F.; Park, D.; Caldwell, D.G.; Berselli, G.; Ortiz, J. State of the Art in Wearable Wrist Exoskeletons Part I: Background Needs and Design Requirements. *Machines* 2023, *11*, 458, doi:10.3390/machines11040458.
3. Pitzalis, R.F.; Park, D.; Caldwell, D.G.; Berselli, G.; Ortiz, J. State of the Art in Wearable Wrist Exoskeletons Part II: A Review of Commercial and Research Devices. *Machines* 2023, *12*, 21, doi:10.3390/machines12010021.
4. Scotto Di Luzio, F.; Cordella, F.; Bravi, M.; Santacaterina, F.; Bressi, F.; Sterzi, S.; Zollo, L. Modification of Hand Muscular Synergies in Stroke Patients after Robot-Aided Rehabilitation. *Applied Sciences* 2022, *12*, 3146, doi:10.3390/app12063146.
5. Krebs, H.I.; Hogan, N.; Volpe, B.T.; Aisen, M.L.; Edelstein, L.; Diels, C. Overview of Clinical Trials with MIT-MANUS: A Robot-Aided Neuro-Rehabilitation Facility. *THC* 1999, *7*, 419–423, doi:10.3233/THC-1999-7606.
6. Narayan, J.; Kalita, B.; Dwivedy, S.K. Development of Robot-Based Upper Limb Devices for Rehabilitation Purposes: A Systematic Review. *Augment Hum Res* 2021, *6*, 4, doi:10.1007/s41133-020-00043-x.
7. Garcia, G.F.; Gonçalves, R.S.; Carbone, G. A Review of Wrist Rehabilitation Robots and Highlights Needed for New Devices. *Machines* 2024, *12*, 315, doi:10.3390/machines12050315.
8. Abarca, V.E.; Elias, D.A. A Review of Parallel Robots: Rehabilitation, Assistance, and Humanoid Applications for Neck, Shoulder, Wrist, Hip, and Ankle Joints. *Robotics* 2023, *12*, 131, doi:10.3390/robotics12050131.
9. Van Eck, N.J.; Waltman, L. Software Survey: VOSviewer, a Computer Program for Bibliometric Mapping. *Scientometrics* 2010, *84*, 523–538, doi:10.1007/s11192-009-0146-3.
10. Maciejasz, P.; Eschweiler, J.; Gerlach-Hahn, K.; Jansen-Troy, A.; Leonhardt, S. A Survey on Robotic Devices for Upper Limb Rehabilitation. *J NeuroEngineering Rehabil* 2014, *11*, 3, doi:10.1186/1743-0003-11-3.
11. Vasseur, D.; Ipakchian Askari, S.; Suijkerbuijk, S.; Nap, H.H.; IJsselsteijn, W. Sensory, Affective, and Social Experiences with Haptic Devices in Intramural Care Practice. *Nursing Reports* 2024, *14*, 230–253, doi:10.3390/nursrep14010019.
12. Jafar, N.; Huriyati, E.; Haryani; Lazuardi, L.; Setyawati, A. Exploring the Coach-Client Interaction of Virtual Health Coaching Conducted in Patients with Type 2 Diabetes Mellitus: A Scoping Review. *Diabetes & Metabolic Syndrome: Clinical Research & Reviews* 2023, *17*, 102787, doi:10.1016/j.dsx.2023.102787.
13. Haddaway, N.R.; Page, M.J.; Pritchard, C.C.; McGuinness, L.A. *PRISMA2020* : An R

Package and Shiny App for Producing PRISMA 2020-compliant Flow Diagrams, with Interactivity for Optimised Digital Transparency and Open Synthesis. *Campbell Systematic Reviews* 2022, *18*, e1230, doi:10.1002/cl2.1230.

14. Ridremont, T.; Singh, I.; Bruzek, B.; Erel, V.; Jamieson, A.; Gu, Y.; Merzouki, R.; Wijesundara, M.B.J. Soft Robotic Bilateral Rehabilitation System for Hand and Wrist Joints. *Machines* 2024, *12*, 288, doi:10.3390/machines12050288.

15. Ridremont, T.; Singh, I.; Bruzek, B.; Jamieson, A.; Gu, Y.; Merzouki, R.; Wijesundara, M.B.J. Pneumatically Actuated Soft Robotic Hand and Wrist Exoskeleton for Motion Assistance in Rehabilitation. *Actuators* 2024, *13*, 180, doi:10.3390/act13050180.

16. Gupta, A.; Singh, A.; Verma, V.; Mondal, A.K.; Gupta, M.K. Developments and Clinical Evaluations of Robotic Exoskeleton Technology for Human Upper-Limb Rehabilitation. *Advanced Robotics* 2020, *34*, 1023–1040, doi:10.1080/01691864.2020.1749926.

17. Jeong, J.; Yasir, I.B.; Han, J.; Park, C.H.; Bok, S.-K.; Kyung, K.-U. Design of Shape Memory Alloy-Based Soft Wearable Robot for Assisting Wrist Motion. *Applied Sciences* 2019, *9*, 4025, doi:10.3390/app9194025.

18. Jeong, J.; Hyeon, K.; Han, J.; Park, C.H.; Ahn, S.-Y.; Bok, S.-K.; Kyung, K.-U. Wrist Assisting Soft Wearable Robot With Stretchable Coolant Vessel Integrated SMA Muscle. *IEEE/ASME Trans. Mechatron.* 2022, *27*, 1046–1058, doi:10.1109/TMECH.2021.3078472.

19. Nobaveh, A.A.; Caasenbrood, B. Design Feasibility of an Energy-Efficient Wrist Flexion-Extension Exoskeleton Using Compliant Beams and Soft Actuators. In Proceedings of the 2022 International Conference on Rehabilitation Robotics (ICORR); IEEE: Rotterdam, Netherlands, July 25 2022; pp. 1–6.

20. Chiaradia, D.; Tiseni, L.; Xiloyannis, M.; Solazzi, M.; Masia, L.; Frisoli, A. An Assistive Soft Wrist Exosuit for Flexion Movements With an Ergonomic Reinforced Glove. *Front. Robot. AI* 2021, *7*, 595862, doi:10.3389/frobt.2020.595862.

21. Syafeeq Lone, S.; Zainul Azlan, N.; Kamarudzaman, N. Soft Pneumatic Exoskeleton for Wrist and Thumb Rehabilitation. *IJRCS* 2021, *1*, 440–452, doi:10.31763/ijrcs.v1i4.447.

22. Liu, Y.-C.; Takeda, Y. Kineto-Static Analysis of a Compact Wrist Rehabilitation Robot Including the Effect of Human Soft Tissue to Compensate for Joint Misalignment. In *ROMANSY 23 - Robot Design, Dynamics and Control*; Venture, G., Solis, J., Takeda, Y., Konno, A., Eds.; CISM International Centre for Mechanical Sciences; Springer International Publishing: Cham, 2021; Vol. 601, pp. 321–329 ISBN 978-3-030-58379-8.

23. Xu, Y. Design and Simulation of a Soft Robotic Device for Wrist Rehabilitation. In Proceedings of the 2020 3rd International Conference on Advanced Electronic Materials, Computers and Software Engineering (AEMCSE); IEEE: Shenzhen, China, April 2020; pp. 697–701.

24. Li, N.; Yang, T.; Yang, Y.; Yu, P.; Xue, X.; Zhao, X.; Song, G.; Elhajj, I.H.; Wang, W.; Xi, N.; et al. Bioinspired Musculoskeletal Model-Based Soft Wrist Exoskeleton for Stroke Rehabilitation. *J Bionic Eng* 2020, *17*, 1163–1174, doi:10.1007/s42235-020-0101-9.

25. Wang, J.; Liu, Z.; Fei, Y. Design and Testing of a Soft Rehabilitation Glove Integrating Finger and Wrist Function. *Journal of Mechanisms and Robotics* 2019, *11*, 011015, doi:10.1115/1.4041789.

26. Ang, B.W.K.; Yeow, C.-H. Design and Characterization of a 3D Printed Soft Robotic Wrist Sleeve with 2 DoF for Stroke Rehabilitation. In Proceedings of the 2019 2nd IEEE International Conference on Soft Robotics (RoboSoft); IEEE: Seoul, Korea (South), April 2019; pp. 577–582.

27. Choi, H.; Kang, B.B.; Jung, B.-K.; Cho, K.-J. Exo-Wrist: A Soft Tendon-Driven Wrist-Wearable Robot With Active Anchor for Dart-Throwing Motion in Hemiplegic Patients. *IEEE Robot. Autom. Lett.* 2019, *4*, 4499–4506, doi:10.1109/LRA.2019.2931607.

28. Bartlett, N.W.; Lyau, V.; Raiford, W.A.; Holland, D.; Gafford, J.B.; Ellis, T.D.; Walsh, C.J. A Soft Robotic Orthosis for Wrist Rehabilitation1. *Journal of Medical Devices* 2015, *9*, 030918, doi:10.1115/1.4030554.

29. Andrikopoulos, G.; Nikolakopoulos, G.; Manesis, S. Design and Development of an Exoskeletal Wrist Prototype via Pneumatic Artificial Muscles. *Meccanica* 2015, *50*, 2709–2730, doi:10.1007/s11012-015-0199-8.

30. Wang, Z.; Cai, Z.; Cui, L.; Pang, C. Structure Design And Analysis Of Kinematics Of An Upper-Limbed Rehabilitation Robot. *MATEC Web Conf.* 2018, *232*, 02033, doi:10.1051/matecconf/201823202033.

31. Zeiaee, A.; Soltani-Zarrin, R.; Langari, R.; Tafreshi, R. Design and Kinematic Analysis of a Novel Upper Limb Exoskeleton for Rehabilitation of Stroke Patients. In Proceedings of the 2017 International Conference on Rehabilitation Robotics (ICORR); IEEE: London, July 2017; pp. 759–764.
32. Hu, R.; Chen, X.; Huang, C.; Cao, S.; Zhang, X.; Chen, X. Elbow-Flexion Force Estimation during Arm Posture Dynamically Changing between Pronation and Supination. *J. Neural Eng.* 2019, *16*, 066005, doi:10.1088/1741-2552/ab2e18.
33. Eschweiler, J.; Li, J.; Quack, V.; Rath, B.; Baroncini, A.; Hildebrand, F.; Migliorini, F. Anatomy, Biomechanics, and Loads of the Wrist Joint. *Life* 2022, *12*, 188, doi:10.3390/life12020188.
34. Rainbow, M.J.; Wolff, A.L.; Crisco, J.J.; Wolfe, S.W. Functional Kinematics of the Wrist. *J Hand Surg Eur Vol* 2016, *41*, 7–21, doi:10.1177/1753193415616939.
35. Akhbari, B.; Morton, A.M.; Shah, K.N.; Molino, J.; Moore, D.C.; Weiss, A.C.; Wolfe, S.W.; Crisco, J.J. Proximal-distal Shift of the Center of Rotation in a Total Wrist Arthroplasty Is More than Twice of the Healthy Wrist. *Journal Orthopaedic Research* 2020, *38*, 1575–1586, doi:10.1002/jor.24717.
36. Laulan, J.; Marteau, E.; Bacle, G. Wrist Osteoarthritis. *Orthopaedics & Traumatology: Surgery & Research* 2015, *101*, S1–S9, doi:10.1016/j.otsr.2014.06.025.
37. Santuz, A.; Ekizos, A.; Janshen, L.; Baltzopoulos, V.; Arampatzis, A. On the Methodological Implications of Extracting Muscle Synergies from Human Locomotion. *Int. J. Neur. Syst.* 2017, *27*, 1750007, doi:10.1142/S0129065717500071.
38. Eschweiler, J.; Stromps, J.-P.; Fischer, M.; Schick, F.; Rath, B.; Pallua, N.; Radermacher, K. Development of a Biomechanical Model of the Wrist Joint for Patient-Specific Model Guided Surgical Therapy Planning: Part 1. *Proc Inst Mech Eng H* 2016, *230*, 310–325, doi:10.1177/0954411916632791.
39. M3 Ball Joint Rod Ends Available online: https://www.revrobotics.com/M3-Ball-Joint-Rod-Ends/ (accessed on 30 July 2024).
40. Petruse, R.E.; Vlad, S.M. Optimizing Manual Assembly Operations: Ergonomics Analysis and Human-Robot Collaboration. *Acta Universitatis Cibiniensis. Technical Series* 2023, *75*, 1–13, doi:10.2478/aucts-2023-0001.
41. Swanson, E.C.; Weathersby, E.J.; Cagle, J.C.; Sanders, J.E. Evaluation of Force Sensing Resistors for the Measurement of Interface Pressures in Lower Limb Prosthetics. *Journal of Biomechanical Engineering* 2019, *141*, 101009, doi:10.1115/1.4043561.
42. Conformable TactArray Flexible Sensors Available online: https://pressureprofile.com/tactarray/conformable-tactarray (accessed on 30 July 2024).
43. Eschweiler, J.; Praster, M.; Quack, V.; Michalik, R.; Hildebrand, F.; Rath, B.; Migliorini, F. Musculoskeletal Modeling of the Wrist via a Multi Body Simulation. *Life* 2022, *12*, 581, doi:10.3390/life12040581.
44. Overview of Materials for Acrylonitrile Butadiene Styrene (ABS), Extruded Available online: https://www.matweb.com/search/DataSheet.aspx?MatGUID=3a8afcddac864d4b8f58d40570d2e5aa&ckck=1 (accessed on 30 July 2024).
45. Rusu, D.-M.; Mândru, S.-D.; Biriş, C.-M.; Petraşcu, O.-L.; Morariu, F.; Ianosi-Andreeva-Dimitrova, A. Soft Robotics: A Systematic Review and Bibliometric Analysis. *Micromachines* 2023, *14*, 359, doi:10.3390/mi14020359.